

Enhanced absorption in silicon nanocone arrays for photovoltaics

Baomin Wang and Paul W Leu

Department of Industrial Engineering, University of Pittsburgh, Pittsburgh, PA 15261, USA

E-mail: pleu@pitt.edu


Received 29 November 2011, in final form 5 February 2012

Published 27 April 2012

Online at stacks.iop.org/Nano/23/194003

Abstract

Silicon nanowire arrays have been shown to demonstrate light trapping properties and promising potential for next-generation photovoltaics. In this paper, we performed systematic and detailed simulation studies on the optical properties of silicon nanocone arrays as compared to nanowires arrays. Nanocone arrays were found to have significantly improved solar absorption and efficiencies over nanowire arrays. Detailed simulations revealed that nanocones have superior absorption due to reduced reflection from their smaller tip and reduced transmission from their larger base. The enhanced efficiencies of silicon nanocone arrays were found to be insensitive to tip diameter, which should facilitate their fabrication. Breaking the vertical mirror symmetry of nanowires results in a broader absorption spectrum such that overall efficiencies are enhanced. We also evaluated the electric field intensity, carrier generation and angle-dependent optical properties of nanocones and nanowires to offer further physical insight into their light trapping properties.

 Online supplementary data available from stacks.iop.org/Nano/23/194003/mmedia

(Some figures may appear in colour only in the online journal)

1. Introduction

Silicon is a naturally abundant, stable, non-toxic material that has been used extensively for semiconductor devices so that its processing and manufacturing is well developed. While silicon has an almost-ideal bandgap for single p–n junction photovoltaics, its infrared absorption is poor. Silicon has absorption lengths $>6 \mu\text{m}$ for photons in the infrared region (energy $E < 1.7 \text{ eV}$) and absorption lengths $>200 \mu\text{m}$ for photons with wavelength $>1000 \text{ nm}$ ($E < 1.2 \text{ eV}$). Typical single-crystalline silicon photovoltaics are thus usually several hundred microns thick to absorb sunlight effectively. These silicon solar cells require costly manufacturing processes such as purification, crystallization and wafer slicing in order to ensure that generated carriers are collected efficiently. Light trapping helps address this issue by increasing the distance photons travel in the silicon before escaping to increase absorption and efficiencies for a particular active layer thickness. Manufacturing costs are reduced because less silicon and poorer quality silicon may be used. Poorer quality silicon with smaller minority carrier

diffusion lengths may be used because charge carriers have to diffuse over smaller distances in order to be collected.

A variety of structures have been investigated for utilizing light trapping to increase absorption in thin film silicon photovoltaics such as diffraction gratings [1], grating couplers [2], photonic crystals [3–6] and random surface textures [7, 8]. These structures contain features that are the same size or smaller than the wavelength of light, such that conventional geometrical light trapping limits (the Yablonovitch or Lambertian limit [9, 10]) are no longer applicable. Much research has focused on silicon nanowires, which have been demonstrated as a promising active layer material for next-generation solar cells [11–20]. Nanowires may orthogonalize light absorption and carrier collection processes to facilitate high optical absorption and efficient collection of photogenerated carriers [21]. Furthermore, nanowires have demonstrated light trapping properties, where their absorption is enhanced over that of planar silicon [11–13, 19]. These structures may also be deposited on low-cost or flexible substrates using chemical vapor deposition or contact transfer methods [22].

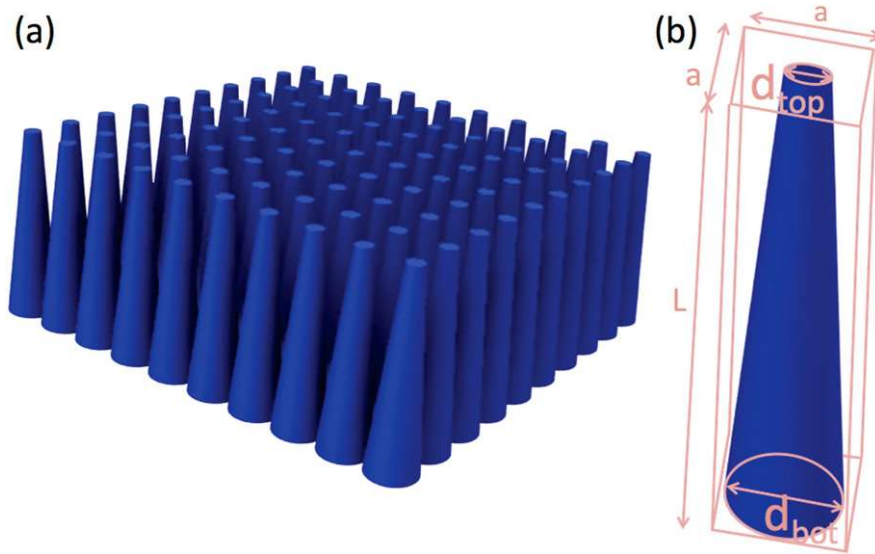


Figure 1. (a) Schematic of the silicon nanocone array structure. (b) The parameters for the array are the length L , the period a , the top diameter d_{top} and the bottom diameter d_{bot} .

Recently, silicon nanocones or tapered nanowires have been experimentally fabricated by metal-assisted electroless etching [23] and a Langmuir–Blodgett assembly and etching technique [24, 25]. These structures have been suggested as candidates for solar cells due to reduced reflection over a broad range of wavelengths through a graded effective refractive index. While experiments have suggested the promise of this new nanostructure for next-generation photovoltaics, there have yet to be any detailed simulation studies. In this paper, we report on detailed numerical investigations of the optical properties and solar conversion efficiencies of nanocone solar cells for a variety of geometries and compare them to nanowire arrays. We found significant enhancements to absorption and conversion efficiencies in silicon nanocone arrays.

2. Methods

Figure 1 shows the schematic of the silicon nanocone arrays studied. The parameters of the structure are the length L , the period a of the square lattice, and the top diameter d_{top} and the bottom diameter d_{bot} . We employed the finite difference time domain method for solving Maxwell's equations. This method is well suited for the computation of the energy-dependent transmission $T(E)$, reflection $R(E)$ and absorption spectra $A(E)$. In order to evaluate the absorption performance of silicon nanocone solar cells across the solar spectrum, we calculated the ultimate efficiency from

$$\eta = \frac{\int_{E_g}^{\infty} I(E)A(E)\frac{E_g}{E} dE}{\int_0^{\infty} I(E) dE} \quad (1)$$

where E is the photon energy, E_g is the bandgap of crystalline silicon, $I(E)$ is the solar irradiance under the global 37° tilt Air Mass 1.5 spectrum [26] and $A(E)$ is the absorption [27]. The bandgap $E_g = 1.12$ eV for crystalline silicon. The

ultimate efficiency describes the efficiency of the cell where each photon absorbed produces one electron–hole pair, and these carriers are collected without recombination such as when the temperature of the cell is 0 K. We evaluated the optical properties over the entire energy range of the solar spectrum from $E = 0.3$ to 4.4 eV (wavelengths from 4000 to 280 nm). The optical constants for silicon were taken from experimental measurement results in Palik's Handbook of Optical Constants of Solids [28]. A plot of the index of refraction is shown in supplementary data figure S1 (available at stacks.iop.org/Nano/23/194003/mmedia). We utilized a uniform mesh of $20 \text{ nm} \times 20 \text{ nm} \times 20 \text{ nm}$ where the ultimate efficiency was found to have converged within 1%. Perfectly matched layer boundary conditions were used for the upper and lower boundary of the simulation cell [29], while appropriate boundary conditions were used for the side boundaries to model the periodic nature of the arrays.

3. Results and discussion

In our studies, we focused on a variety of different geometries for silicon nanocones with fixed pitch $a = 600$ nm, since this pitch has been shown to be optimal for silicon nanowires [12, 30]. The efficiencies of nanocones and nanowires were compared at a variety of lengths, though we initially focused on nanocones and nanowires with length $L = 2.33 \mu\text{m}$. Figure 2 shows the results of these studies. Figure 2(a) shows the ultimate efficiency as a function of diameter d for vertical nanowire arrays. The optimal ultimate efficiency was found to be 29.8% when $d = 560$ nm or the fill fraction $f = 0.68$. The ultimate efficiency is $>27\%$ when $d > 400$ nm (or $f > 0.35$). This efficiency is impressive and has been shown to be superior to thin films of the same active layer thickness with optimized antireflection coatings [12].

However, significant superior ultimate efficiencies may be achieved with silicon nanocones. Figure 2(b) utilizes a

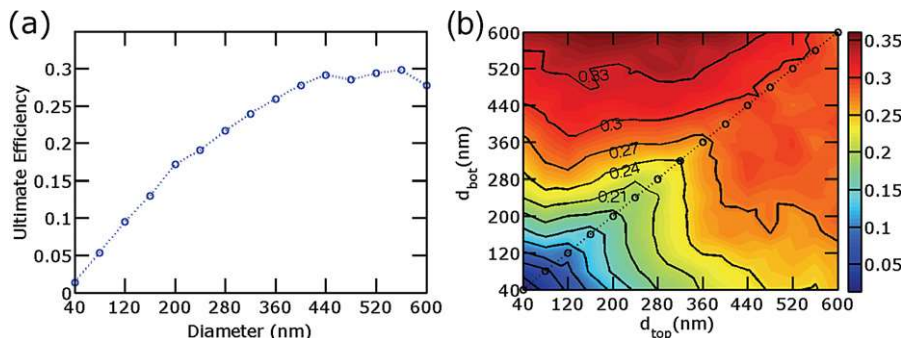


Figure 2. Ultimate efficiency of silicon nanowires and nanocones where the length $L = 2.33 \mu\text{m}$ and pitch $a = 600 \text{ nm}$. (a) Ultimate efficiency as a function of the diameter d for nanowire arrays. (b) Contour plot of ultimate efficiency for silicon nanocone arrays as a function of d_{top} and d_{bot} . The dotted line indicates $d_{\text{top}} = d_{\text{bot}}$, which is the geometry of nanowire arrays.

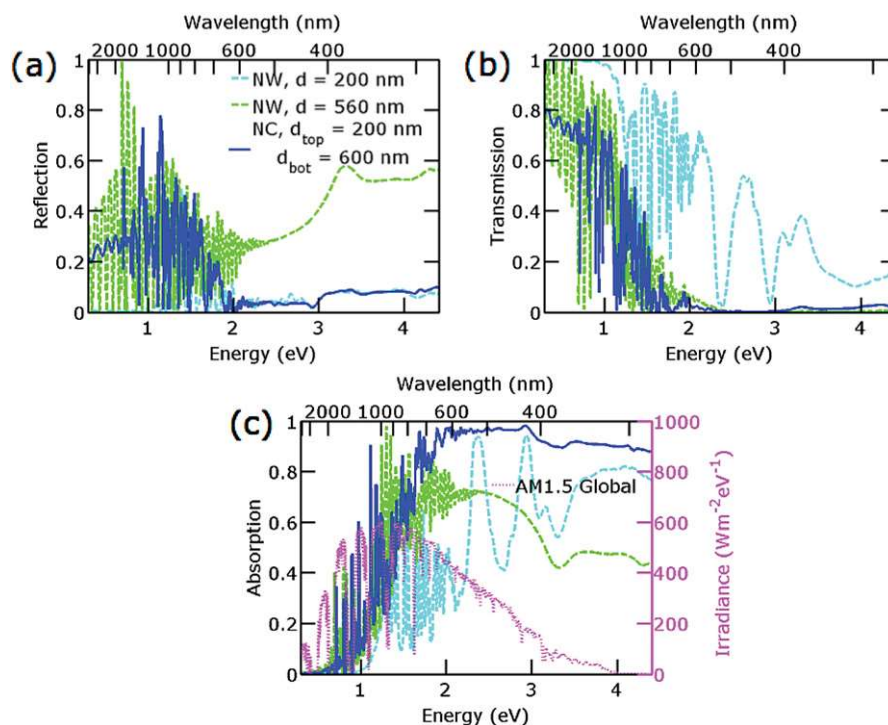


Figure 3. Optical properties of three different silicon nanostructures: single-diameter nanowire (NW) arrays with $d = 200$ and 560 nm and nanocone (NC) arrays with $d_{\text{top}} = 200 \text{ nm}$ and $d_{\text{bot}} = 600 \text{ nm}$. (a)–(c) show the reflectance, transmittance and absorption, respectively. The irradiance of the Air Mass 1.5 solar spectrum is shown in the right y axis of (c).

contour plot to illustrate the dependence of ultimate efficiency on the geometry of the silicon nanocone. The parameters d_{top} and d_{bot} were varied from 40 to 600 nm in 40 nm increments and values between data points were obtained by triangle-based linear interpolation. Nanowires are special instances of nanocones, where the diameter is constant across the entire length of the structure or $d = d_{\text{top}} = d_{\text{bot}}$, and a dotted line is plotted in the contour plot to indicate this geometry. In our studies, we found that nanocones with $d_{\text{top}} < d_{\text{bot}}$ may be utilized to achieve better ultimate efficiencies than nanowires. The optimal ultimate efficiency was 36.2% for $d_{\text{top}} = 200 \text{ nm}$ and $d_{\text{bot}} = 600 \text{ nm}$, which is about 22% higher than that of the optimal single-diameter nanowire array. One of the advantages of nanocones that may be observed from the contour plot is that the ultimate efficiency

is not particularly sensitive to d_{top} . For example, ultimate efficiencies greater than 31% may be achieved for nanowires with $d_{\text{bot}} = 600 \text{ nm}$ and $d_{\text{top}} < 520 \text{ nm}$. Optimal nanocone structures are robust in deviations from idealized geometries and not particularly sensitive to variation or imperfections in manufacturing techniques.

Based on the results of our investigations into different nanocone and nanowire geometries, we chose several representative nanowire and nanocone systems to compare their reflection, transmission and absorption spectra. Figure 3 illustrates the (a) reflection, (b) transmission and (c) absorption as a function of energy for three representative systems. The optimum efficiency nanowire with $d = 560 \text{ nm}$ and optimum nanocone with $d_{\text{top}} = 200 \text{ nm}$ and $d_{\text{bot}} = 600 \text{ nm}$ are shown. Furthermore, we plot the spectra of the nanowire

Table 1. Absorption in different wavelength regimes. The infrared and total solar regions are calculated for those portions of the regions that are above the silicon bandgap ($E > 1.12$ eV).

Spectrum region	NW, $d = 200$ nm	NW, $d = 560$ nm	NC, $d_{\text{top}} = 200$ nm, $d_{\text{bot}} = 600$ nm
Infrared (%)	21	52	54
Ultraviolet (%)	67	46	91
Visible (%)	45	69	93
Total solar (%)	35	61	74

with $d = 200$ nm, since this is the top diameter of the optimal nanocone. In figure 3(c), the absorption was calculated from $A(E) = 1 - R(E) - T(E)$ and the global 37° tilt Air Mass 1.5 spectrum is shown on the right y axis. Single-diameter nanowire systems exhibit a tradeoff between reflection and transmission. Smaller-diameter nanowires such as the one illustrated with $d = 200$ nm have less reflection because there is less fill factor or area for light to reflect off the top of the nanowires. However, they also have higher transmission throughout the entire solar spectrum because there is less silicon to absorb the light. On the other hand, larger diameter nanowire arrays, such as the optimal single-diameter system with $d = 560$ nm, exhibit higher reflection due to higher fill factor and smaller transmission since there is more material to absorb the light. Larger-diameter nanowire arrays have better absorption in the infrared range, but poorer absorption in the ultraviolet range.

Silicon nanocone arrays address the tradeoff between reflection and transmission with a smaller d_{top} and a larger d_{bot} . The optimal silicon nanocone array, with $d_{\text{top}} = 200$ nm and $d_{\text{bot}} = 600$ nm, especially in the visible and ultraviolet range, has reflection about the same of the small single-diameter nanowire array with $d = 200$ nm. The larger base results in a transmission that is almost zero in the visible and ultraviolet regime. In the infrared range, the silicon nanocone array has absorption characteristics comparable to that of the best single-diameter nanowire array. However, in the visible and ultraviolet range, the absorption is significantly improved with absorption from about 80% to 95% compared to 40% to 80% for the best single-diameter structures. Table 1 lists the fraction of photons absorbed in different regions of the solar spectrum for these three representative nanowire and nanocone systems. The visible region is from 380 to 740 nm (1.7–3.3 eV), the ultraviolet region is from 280 to 400 nm (3.1–4.4 eV), and the infrared region (above the silicon bandgap) is from 740 to 1100 nm (1.1–1.7 eV). The total solar region shown only includes the range above the silicon bandgap energy from 280 to 1100 nm (1.1–4.4 eV). The silicon nanocone arrays have enhanced absorption compared to silicon nanowire arrays over the entire spectral range due to antireflection and low transmission in the visible and ultraviolet ranges.

In order to understand the propagation of light in the nanowire and nanocone arrays, we simulated the electrical field intensity $|\mathbf{E}(\mathbf{r}, E)|^2$ and calculated the generation rate

within the arrays from

$$G(\mathbf{r}, E) = \frac{\epsilon_i(E)|\mathbf{E}(\mathbf{r}, E)|^2}{2\hbar} \quad (2)$$

where $\epsilon_i(E)$ is the imaginary part of the dielectric constant, \hbar is the reduced Planck constant and $\mathbf{E}(\mathbf{r}, E)$ is the energy- and position-dependent electric field. By normalizing this quantity over the simulation power, and integrating over the solar spectrum energies as weighted by the solar irradiance $I(E)$, we obtain the solar-spectrum-weighted generation rate as plotted in figure 4. Figure 4 shows the cross-sectional (a) solar-spectrum-weighted electrical field intensity $|\mathbf{E}(\mathbf{r})|^2$ and (b) solar-spectrum-weighted generation rate $G(\mathbf{r})$ of the three representative nanowire and nanocone arrays for normal incident light integrated over photon energies $E = 0.83$ – 2.75 eV (or wavelengths $\lambda = 1500$ – 450 nm). This energy range encompasses about 86% of the power density available for absorption by silicon. The electric field of the incoming electromagnetic wave was out of the plane of the paper in these simulations. The left column illustrates single-diameter nanowire arrays with $d = 200$ nm, the middle column shows the optimal single-diameter nanowire arrays with $d = 560$ nm and the right column illustrates the optimal nanocone arrays with $d_{\text{top}} = 200$ nm and $d_{\text{bot}} = 600$ nm. Dotted white lines indicate the edges of these silicon nanostructures.

In the 200 nm diameter nanowire arrays, a large portion of the electromagnetic (EM) waves propagates outside the Si nanowire. The EM waves decay in the radial direction, such that a significant portion of the carrier generation is near the surface. While the reflection is low in these nanowire arrays due to their small diameter, the transmission is also higher since there is less silicon to absorb the light, and the intensity of the electric field can be seen to be still significant near the bottom of the nanowire. In the 560 nm diameter nanowire arrays, most of the carrier generation occurs in the center of the nanowire away from the nanowire surface. There is more silicon in the larger-diameter nanowire arrays to absorb the EM waves, such that the electric field intensity is close to zero at the bottom of the nanowire. However, because of the large fill factor or the large top of the nanowire, the reflection is substantial.

In the nanocone array, the EM field is seen to propagate further into the structure. The small diameter d_{top} results in smaller reflection, while the larger base contains more silicon to absorb the light. The electric field intensity is seen to decay to very small values near the bottom of the nanocone array, indicative of small transmission. The nanocone arrays have the advantage that the carrier generation, similar to the larger-diameter nanowires, occurs near the center of the nanocones, such that carriers are less likely to be affected by surface recombination. Furthermore, the carrier generation is more uniform along the length of the nanowire, such that photoexcited carriers are less likely to recombine, since the recombination rate is directly proportional to the local excess concentration of electrons and holes.

Guided resonance modes (also called leaky-mode resonances) have been shown to play a significant role in light

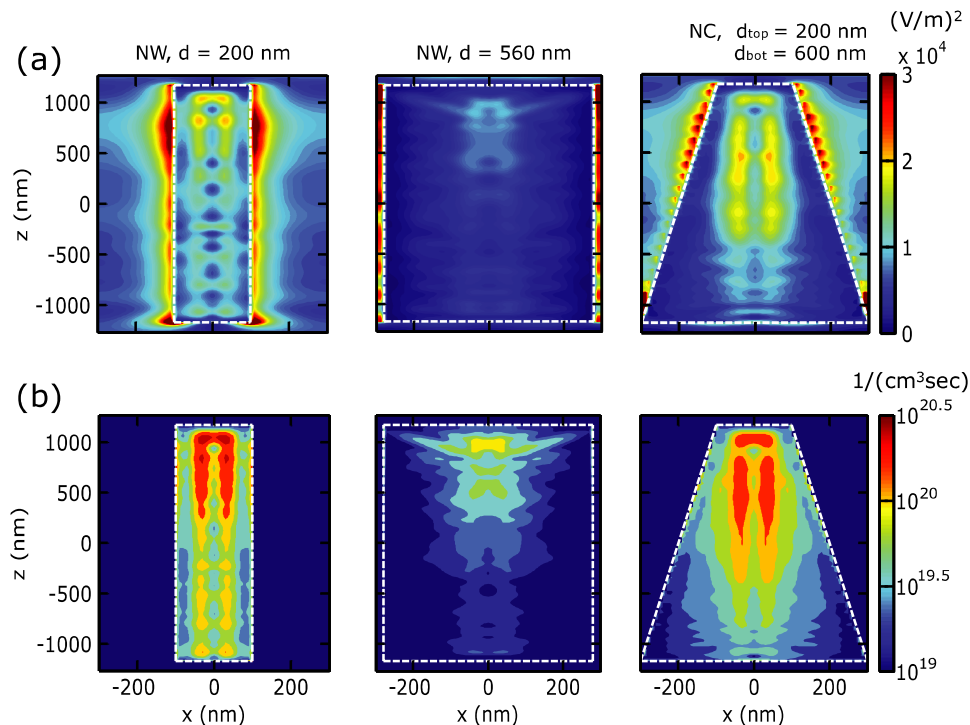


Figure 4. The (a) solar-spectrum-weighted electrical field intensity $|\mathbf{E}(\mathbf{r})|^2$ and (b) solar-spectrum-weighted generation rate $G(\mathbf{r})$ for three representative silicon nanowires and nanocones. From left to right, the systems shown are nanowire arrays with $d = 200$ nm, nanowire arrays with $d = 560$ nm and nanocone arrays with $d_{\text{top}} = 200$ nm and $d_{\text{bot}} = 600$ nm.

absorption by nanowires [12, 31]. Nanowire arrays exhibit a mirror-symmetry plane at $z = 0$, such that modes must be either symmetric or antisymmetric about the plane. TE-like modes are odd with respect to z and TM-like modes are even with respect to z . Distinct peaks may be seen in the absorption spectrum of nanowire arrays corresponding to the coupling of incident light with these guided resonance modes. These guided resonance modes may be tuned for the detection of particular energies or frequencies in photodetectors for example [31]. In photovoltaics, however, it is generally desirable for absorption to occur over a broad range of energies. By tapering the nanowires or forming nanocones, the mirror symmetry is removed and the absorption spectrum is broadened such that the overall absorption may be enhanced over that of nanowire arrays.

In order to evaluate the performance of non-tracking photovoltaics, we simulated the angle-dependent optical properties of the optimal silicon nanocone array as compared to the optimal nanowire array. The ultimate efficiency is plotted as a function of the zenith angle θ from 0° to 55° in figure 5. We found little variation in absorption with the azimuthal angle. The results show that, for both transverse-electric (TE) polarization and transverse-magnetic (TM) polarization, the ultimate efficiency of silicon nanocone arrays is higher than that of nanowire arrays. The difference between the nanocone and nanowire array is larger at smaller angles, but becomes smaller at higher angles. When evaluating the different spectra, we found that the integrated transmission of the nanocone and nanowire array was about the same at various angles. For higher incident zenith angles,

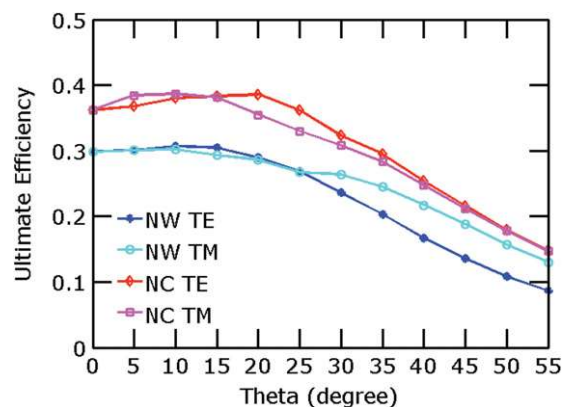


Figure 5. Relationship between ultimate efficiency and zenith angle θ of optimal nanowire and nanocone arrays for TE and TM modes.

the integrated reflection rose in both the nanowire arrays and the nanocone arrays. Above 25° , the integrated reflection in both structures rose quickly, such that the total absorption and hence the efficiency dropped. Above 40° , the difference in reflection between the two structures became smaller.

Finally, we considered different geometries of nanocone and nanowire arrays for a wide range of lengths. In addition to the length $L = 2330$ nm, we further compared nanocones and nanowires for L from 50 to 10000 nm for fixed pitch $a = 600$ nm. Full contour plots of the ultimate efficiency as a function of d_{top} and d_{bottom} for the different lengths simulated are included in supplementary data figures S2–S4

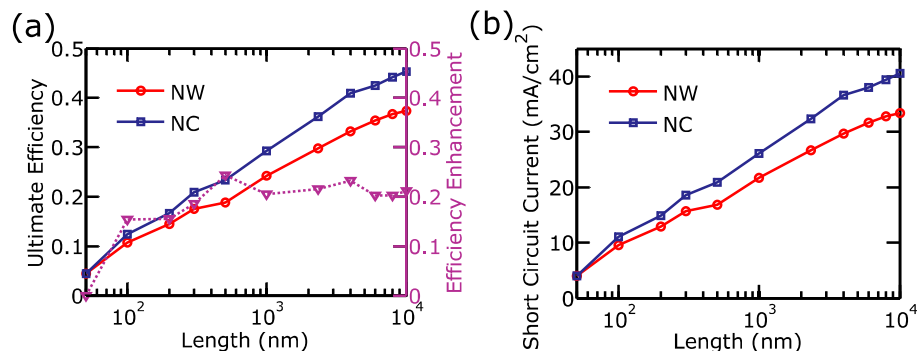


Figure 6. Optimal ultimate efficiency of silicon nanowires and nanocones with different lengths L . The contour plots of ultimate efficiency with different lengths are provided as figures S2–S4 in the supplementary data (available at stacks.iop.org/Nano/23/194003/mmedia).

(available at stacks.iop.org/Nano/23/194003/mmedia). The optimal ultimate efficiency and short circuit current for nanocone and nanowire arrays were obtained from these simulations and plotted in figure 6. The short circuit current, assuming perfect carrier extraction, is calculated from

$$J_{sc} = q \int_0^{\infty} b_s(E)A(E) dE. \quad (3)$$

where $b_s(E)$ is the photon flux density of the solar spectrum. We found that nanocone arrays have better efficiencies and short circuit currents than nanowires across a wide range of lengths. The efficiency enhancement (which is the same as the short circuit current enhancement for perfect carrier extraction) of the optimal nanocone array over the nanowire array is plotted on the right y axis in figure 6. The ultimate efficiency enhancement is greater than 20% for $L > 500$ nm. For the smallest length $L = 50$ nm, the amount of silicon is small such that the best structure is a nanowire with $d = a = 600$ nm. Most of the loss is through transmission, such that nanocones do not have an advantage over nanowires. However, for longer lengths, nanocones have significant advantages over nanowires when d_{top} is less than d_{bot} .

4. Conclusion

In summary, we have studied the optical performances of silicon nanocone arrays for photovoltaic application, and compared them with nanowire arrays across different diameters and lengths. This novel structure can obtain enhanced absorption due to antireflection from the small tip and lower transmission due to the larger base. Nanocones may be fabricated by well-developed techniques, and are not particularly sensitive to specific geometry, which should facilitate their fabrication. We have also evaluated the solar-spectrum-weighted electric field intensity and generation rate in silicon nanocone arrays and determined advantages of nanocone arrays over nanowire arrays in which carriers are photoexcited. Breaking the vertical mirror symmetry of nanowires results in a broader absorption spectrum such that overall efficiencies may be enhanced. These efficiencies are also superior over a broad range of incident angles.

Acknowledgments

This work was supported by a Mascaro Center for Sustainable Innovation Seed Grant. Computing resources were provided by the Center for Simulation and Modeling at the University of Pittsburgh.

References

- [1] Feng N N, Michel J, Zeng L R, Liu J F, Hong C Y, Kimerling L C and Duan X M 2007 *IEEE Trans. Electron Devices* **54** 1926
- [2] Stieglitz H, Senoussaoui N, Zahren C, Haase C and Müller J 2006 *Prog. Photovolt., Res. Appl.* **14** 13
- [3] Bermel P, Luo C Y, Zeng L R, Kimerling L C and Joannopoulos J D 2007 *Opt. Express* **15** 16986
- [4] Chutinan A and John S 2008 *Phys. Rev. A* **78** 023825
- [5] Zhou D and Biswas R 2008 *J. Appl. Phys.* **103** 093102
- [6] Mallick S B, Agrawal M and Peumans P 2010 *Opt. Express* **18** 5691
- [7] Rockstuhl C, Fahr S, Bittkau K, Beckers T, Carius R, Haug F J, Söderström T, Ballif C and Lederer F 2010 *Opt. Express* **18** A335
- [8] Hsu C M, Burkhard F B, McGehee M D and Cui Y 2010 *Nano Res.* **4** 153
- [9] Yablonovitch Y and Cody G 1982 *IEEE Trans. Electron Devices* **29** 300
- [10] Yablonovitch Y 1982 *J. Opt. Soc. Am.* **72** 899
- [11] Kelzenberg M D, Boettcher S W, Petykiewicz J A, Turner-Evans D B, Putnam M C, Warren E L, Spurgeon J M, Briggs R M, Lewis N S and Atwater H A 2010 *Nature Mater.* **9** 239
- [12] Lin C X and Povinelli M L 2009 *Opt. Express* **17** 19371
- [13] Garnett E and Yang P Y 2010 *Nano Lett.* **10** 1082
- [14] Peng K Q, Xu Y, Wu Y, Yan Y J, Lee S T and Zhu J 2005 *Small* **1** 1062
- [15] Tsakalacos L, Balch J, Fronheiser J, Korevaar B A, Sulima O and Rand J 2007 *Appl. Phys. Lett.* **91** 233117
- [16] Stelzner Th, Pietsch M, Andrä G, Falk F, Ose E and Christiansen S 2008 *Nanotechnology* **19** 295203
- [17] Yu K N and Chen J H 2008 *Nanoscale Res. Lett.* **4** 1
- [18] Hu L and Chen G 2007 *Nano Lett.* **7** 3249
- [19] Xie W Q, Oh J I and Shen W Z 2011 *Nanotechnology* **22** 065704
- [20] Fan Z Y, Ruebusch D J, Rathore A A, Kapadia R, Ergen O, Leu P W and Javey A 2009 *Nano Res.* **2** 829

- [21] Kayes B M, Atwater H A and Lewis N S 2005 *J. Appl. Phys.* **97** 114302
- [22] Fan Z Y *et al* 2009 *Nature Mater.* **8** 648
- [23] Jung J Y, Guo Z Y, Jee S W, Um H D, Park K T and Lee J H 2010 *Opt. Express* **18** A286
- [24] Hsu C M, Connor S T, Tang M X and Cui Y 2008 *Appl. Phys. Lett.* **93** 133109
- [25] Zhu J, Yu Z F, Burkhard G F, Hsu C M, Connor S T, Xu Y Q, Wang Q, McGehee M, Fan S H and Cui Y 2009 *Nano Lett.* **9** 279
- [26] Solar spectral irradiance: Air mass 1.5 <http://rredc.nrel.gov/solar/spectra/am1.5/>
- [27] Shockley W and Queisser H J 1961 *J. Appl. Phys.* **32** 510
- [28] Palik D E 1997 *Handbook of Optical Constants of Solids* vol 1 (New York: Academic)
- [29] Berenger J P 1994 *J. Comput. Phys.* **114** 185
- [30] Li J S, Yu H Y, Wong S M, Li X C, Zhang G, Lo P G and Kwong D L 2009 *Appl. Phys. Lett.* **95** 243113
- [31] Cao L Y, White J S, Park J S, Schuller J A, Clemens B M and Brongersma M L 2009 *Nature Mater.* **8** 643